Materials Research Proceedings 34 (2023) 120-126 https://doi.org/10.21741/9781644902691-15

The Influence of Mn Addition on Corrosion Resistance in Secondary Aluminium Alloy AlSi7Mg0.3 after the Heat Treatment

ŠURDOVÁ Zuzana[1,a *], KUCHARIKOVÁ Lenka[1,b], TILLOVÁ Eva[1,c] and CHALUPOVÁ Mária[1,d]

[1]University of Žilina, Faculty of Mechanical Engineering, Department of Materials Engineering, Univerzitná 8215/1, 010 26 Žilina, Slovak Republic

[a] zuzana.surdova@fstroj.uniza.sk *, [b] lenka.kucharikova@fstroj.uniza.sk,
[c] eva.tillova@fstroj.uniza.sk, [d] maria.chalupova@fstroj.uniza.sk

Keywords: AlSi7Mg0.3; Al_5FeSi; Heat Treatment, 3.5% NaCl, Corrosion Resistance

Abstract. This paper aims to study the secondary aluminium alloy AlSi7Mg0.3 with higher Fe content after heat treatment. The addition of Mn is also investigated. The quantitative analysis was performed to evaluate the effect of higher Fe content on the amount and shape of platelet-like Fe-rich intermetallic phases. As a method of corrosion resistance testing an immersion test in 3.5% NaCl was used. This test was done in order to evaluate the influence of higher Fe content and Mn addition in heat-treated AlSi7Mg0.3 alloys. The results show that the Mn addition increases the corrosion resistance of AlSi7Mg0.3 alloys, but not significantly. AlSi7Mg0.3 alloys have numerous uses within the automobile and other sectors.

Introduction

Aluminium alloys have gained widespread use in various industrial applications due to their exceptional properties, such as low density, high thermal conductivity, and good corrosion resistance. Among aluminium alloys, secondary aluminium alloys are particularly attractive due to their low production cost and high recyclability. These alloys are produced by casting processes using recycled aluminium scrap as the raw material [1,2].

AlSi7Mg0.3 alloy is a popular secondary aluminium alloy, which is widely used in various applications such as automotive, aerospace, and construction. It is an Al-Si-Mg-based alloy with a nominal composition of 7.0 wt. % Si and 0.3 wt. % Mg, which gives it good casting properties, high strength, and good corrosion resistance [3,4]. The heat-treatable nature of AlSi7Mg0.3 also enables further improvement of its mechanical properties through solution heat treatment and ageing. Despite its advantages, the presence of Fe and other impurities in the recycled aluminium scrap can negatively impact the microstructure and properties of AlSi7Mg0.3 alloys, thus, requiring careful selection of raw materials and precise control of casting conditions [5-8].

Intermetallic phases play a critical role in determining the mechanical and corrosion properties of the secondary Al-Si-Mg-based AlSi7Mg0.3 alloy. The microstructure of AlSi7Mg0.3 consists of a complex network of intermetallic phases and eutectic structures, which result from the reaction between the solid aluminium matrix and the dispersed silicon particles. The presence and distribution of intermetallic phases significantly affect the properties of the alloy, and therefore, understanding their formation and growth is important for optimizing the properties of the AlSi7Mg0.3 alloy. The intermetallic phases in AlSi7Mg0.3 can be classified into several types, including Fe-rich Al_5FeSi, $Al_{15}(FeMn)_3Si_2$, and Mg_2Si, each with unique chemical and physical properties that contribute to the overall behaviour of the alloy [8-10].

In AlSi7Mg0.3 alloys, an increase in Fe content can have a negative impact on the microstructure and properties of the material. The presence of Fe in these alloys can also result in the formation of undesired phases, such as Fe-rich Al_5FeSi, which can negatively affect the mechanical properties and corrosion resistance of the material. Therefore, controlling the Fe

Materials Research Proceedings 34 (2023) 120-126 https://doi.org/10.21741/9781644902691-15

content and mitigating its negative effects are important considerations in the production and application of said alloys [10-12].

Manganese is an important element added to AlSi7Mg0.3 alloy for the purpose of improving its properties. The addition of Mn has been found to have a significant effect on the microstructure and mechanical properties of the alloy, including enhanced corrosion resistance and improved formability. Mn addition can also alter the precipitation kinetics of intermetallic phases and change the type of phases formed in the alloy [6,13,14].

Secondary AlSi7Mg0.3 aluminium alloy is widely used in various industries such as aerospace, transportation, and construction. In the automotive industry, it is commonly used in wheel production, engine components and other structural parts. The alloy's good mechanical properties and corrosion resistance make it an attractive choice for various engineering applications, including high-temperature high-stress, and high-corrosion environments. The widespread use of this alloy highlights its versatility and adaptability [3,15].

Materials and Methods

The secondary AlSi7Mg0.3 aluminium cast alloy samples being studied were produced by UNEKO spol. s.r.o, Zátor, Czech Republic. They were supplied in the form of circular rods, 300 mm long and 20 mm in diameter (Fig. 1), made by gravity casting into sand moulds treated to prevent liquid metal penetration. A protective spray was applied to improve surface quality.

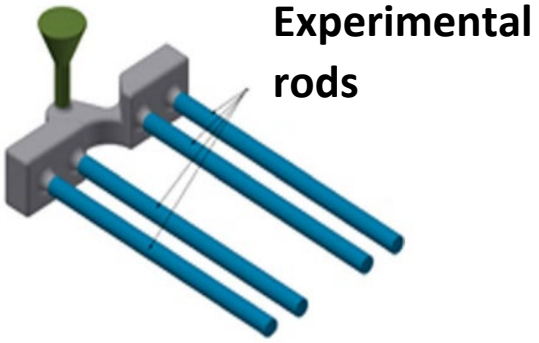

Fig.1. *The casting model of experimental rods.*

To assess the impact on Fe-rich intermetallic phases and corrosion resistance caused by increased Fe content and Mn addition in heat-treated samples, 4 alloys with different Fe contents were cast: 0.123 % Fe (alloy A), 0.454 % Fe (alloy B), 0.679 % Fe (alloy C), and 1.209 % Fe (alloy D). Table 1 displays the chemical composition of the alloys and the calculated critical iron value. Each melt was cast at 750°C and refined at 740-745°C. As a refining salt, ECOSAL AL 113S was used. All experimental bars were subjected to heat treatment T6 – solution annealing at a temperature of 530°C ± 5 °C with a holding time of 7 hours, rapid cooling to a temperature of 50°C and artificial ageing at a temperature of 160°C for 6 hours. These samples were compared to determine whether the heat treatment negates the negative effect of higher Fe content.

Microstructure analysis was performed to understand the connection between microstructure and corrosion resistance, and the impact of heat treatment on the AlSi7Mg0.3 alloys. The samples were prepared using a metallographic process involving grinding with 500 and 1 200-grit Strues SiC paper, followed by polishing with 3 μm diamond paste and Strues Op-S. Chemical etching was done using 0.5% HF and H_2SO_4 to highlight Fe-rich phases. The samples were then observed using a NEOPHOT 32 optical microscope. An optical microscope and NIS Elements 5.2 software were utilized for the quantitative analysis of Fe-rich phases to assess the impact of Fe content Mn

addition and heat treatment (T6) on their length, particularly those in the plate-like (needle) shape. The length of needle-shaped Fe-rich intermetallic phases was measured 50 times on all experimental samples with and without Mn addition.

To study the corrosion resistance of the secondary AlSi7Mg0.3 aluminium alloy, an immersion test using a 3.5% NaCl solution was employed. The specimens for the test were 18 mm in diameter and 10 mm long, with 3 specimens per melt. They were cleaned in distilled water and ethanol, dried with hot air, then weighed with analytical scales, accurately to 4 decimal places, and immersed in the 3.5% NaCl solution for three weeks.

Table 1. *The chemical composition of experimental alloy AlSi7Mg0.3 [wt. %]*

Alloy	Si	Fe	Cu	Mn	Mg	Cr	Zn	Ti	Ga	V	Al	$Fe_{crit.}$
A	7.340	**0.454**	0.021	**0.01**	0.3	0.002	0.02	0.12	0.01	0.01	ball.	0.501
A^{Mn}	7.051	**0.450**	0.021	**0.122**	0.26	0.002	0.02	0.11	0.01	0.01	ball.	0.479
B	7.346	**0.679**	0.0096	**0.01**	0.4	0.002	0.03	0.11	0.01	0.01	ball.	0.501
B^{Mn}	7.039	**0.681**	0.008	**0.337**	0.31	0.002	0.03	0.12	0.01	0.01	ball.	0.478
C	7.340	**1.209**	0.01	**0.01**	0.31	0.002	0.01	0.12	0.01	0.01	ball.	0.501
C^{Mn}	7.212	**1.200**	0.0098	**0.585**	0.28	0.002	0.01	0.12	0.01	0.01	ball.	0.491

To prevent interference with the corrosion process, the samples were positioned in the glass container so that they did not touch each other or the walls. In order to avoid a change in the concentration of 3.5% of NaCl solution and that the electrolyte level remains throughout the duration of the test (3 weeks) constant, distilled water was carefully poured down the sides of the vessel. In the room where the immersion test was carried out, a constant temperature of 20 ± 2 °C was maintained. If the measures described above are not followed, the kinetics may be altered of the corrosion processes and therefore erroneous results.

After the test time had elapsed, the samples were rinsed in distilled water and ethanol, dried with hot air, reweighed, and evaluated gravimetrically. The extent of the corrosion attack was observed using an Olympus Stereo microscope SZX16 and the impact of increased Fe content and Mn addition was evaluated.

Results and Discussion

The microstructure of the alloys studied in this research is displayed in Fig. 2. The standard microstructure of the alloys includes α-phase eutectic (seen as dark Si crystals in α-phase), and various intermetallic phases. Eutectic silicon is seen after heat treatment as small, round particles. The identified intermetallic phases in the alloys include plate-like Al_5FeSi skeleton-like $Al_{15}(FeMn)_3Si_2$ and Mg-rich (Mg_2Si) very fine particles. The needle-like Al_5FeSi phase is fragmented into smaller needles after heat treatment.

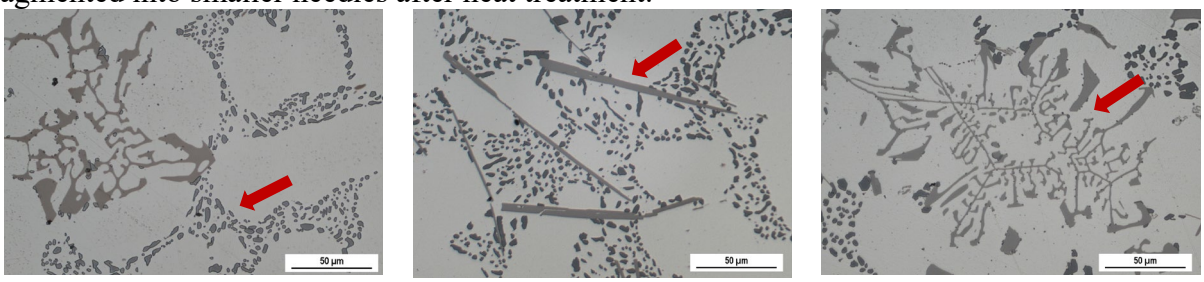

a) eutectic silicon b) Al_5FeSi phase c) $Al_{15}(FeMn)_3Si_2$ phase

Fig.2. *Microstructure of experimental alloys.*

Materials Research Proceedings 34 (2023) 120-126 https://doi.org/10.21741/9781644902691-15

An increase in Fe content usually results in a higher number of Fe-rich needle-like phases in the microstructure and in the growth in their length, but this trend was not seen in the alloys used in this study. The growth of Al_5FeSi phases was not exponential as was expected (Table 2). The highest average length of the Fe-rich phase Al_5FeSi was observed in alloy A. In alloys B and C with increasing iron content, larger acicular phases were not observed. Probably after exceeding 0.5 % iron content, iron no longer has such a negative effect, the phases are rather thicker and shorter. The smallest average length was measured in alloys B^{Mn} and C^{Mn}. This is because these experimental alloys met the Mn/Fe = 1:2 condition (a condition that if met, results in a change in intermetallic morphology from needle-like phases to skeleton-like phases).

Table 2. *The results of the quantitative analysis of experimental alloys*

Alloy	Fe [wt. %]	Mn [wt. %]	Mn/Fe	Minimum length [µm]	Maximum length [µm]	Average length [µm]
Alloy A	0.454	0.01	0.022	7.97	269.16	55.02
Alloy A^{Mn}	0.450	0.122	0.271	15.26	117.41	37.56
Alloy B	0.679	0.01	0.015	6,57	155.32	36.25
Alloy B^{Mn}	0.681	0.337	**0.495**	11.63	75.87	34.52
Alloy C	1.209	0.01	0.008	5.85	141.8	40.57
Alloy C^{Mn}	1.200	0.585	**0.488**	6.01	59.36	17.41

Table 3. *The weight changes of experimental alloys after immersion test [g]*

Sample	A	A^{Mn}	B	B^{Mn}	C	C^{Mn}
Weight loss	-0.0039	-0.0044	-0.0035	-0.0014	-0.0023	-0.0013

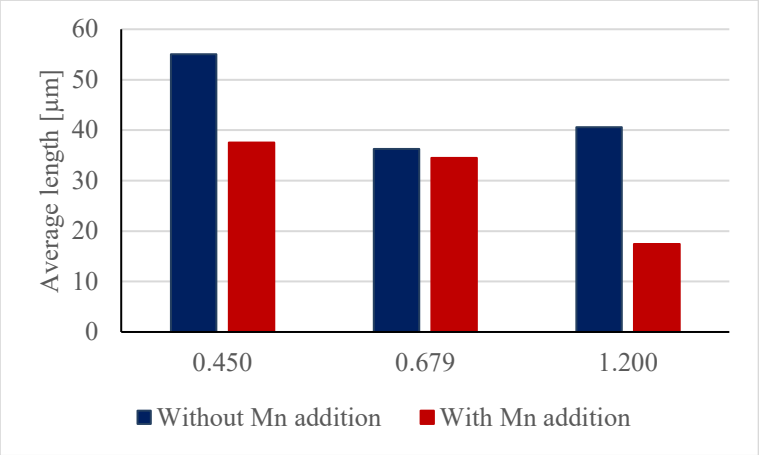

Fig.3. *The effect of Mn addition on the length of Al_5FeSi needles.*

Thus, quantitative analysis proved that in melts, which had Mn addition, there were on average shorter Fe phases, in the form of needles, than in the melts which were without Mn addition, only with increased Fe content. A graph was created to visually compare the average length of Fe phases in the experimental alloys with and without Mn addition (Fig. 3).

The immersion test using 3.5% NaCl was conducted to study the corrosion behaviour of the AlSi7Mg0.3 alloys. After three weeks the samples were removed from the solution and washed, dried, weighed, and evaluated gravimetrically by calculating average mass changes. The gravimetric results are shown in Table 3.

Materials Research Proceedings 34 (2023) 120-126 https://doi.org/10.21741/9781644902691-15

All experimental samples showed weight loss. The immersion test using 3.5% NaCl showed that the addition of Mn enhances corrosion resistance, particularly in alloy B. Nevertheless, it should be noted that the Mn addition does not result in a substantial improvement in corrosion resistance in the alloys studied in this particular corrosion test. Subsequently, a macroscopic examination of the corrosion damage was conducted. The macroscopic evaluation of the surface of the samples after the immersion corrosion test showed the presence of pitting corrosion in all samples examined (Fig.4).

In the experimental alloys after the immersion test, a heterogeneous corrosion attack of the material was preferentially observed. Chloride anions, by passing through the passive layer of the material, cause the formation of a corrosion pit. The pits are formed on the surface of the material, especially where there are various inhomogeneities, and impurities and their formation also occur at grain boundaries, i.e., in the eutectic. The intensity of the corrosion attack of the experimental alloys also depends on whether the alloys are heat treated or not. The change in the morphology of Si particles after heat treatment (the so-called spheroidization of Si) positively affects the dissolution rate of α-phase in the eutectic; it slows it down, compared to alloys in the as-cast state. Therefore, a lower density of corrosion pits can generally be observed in heat-treated alloys.

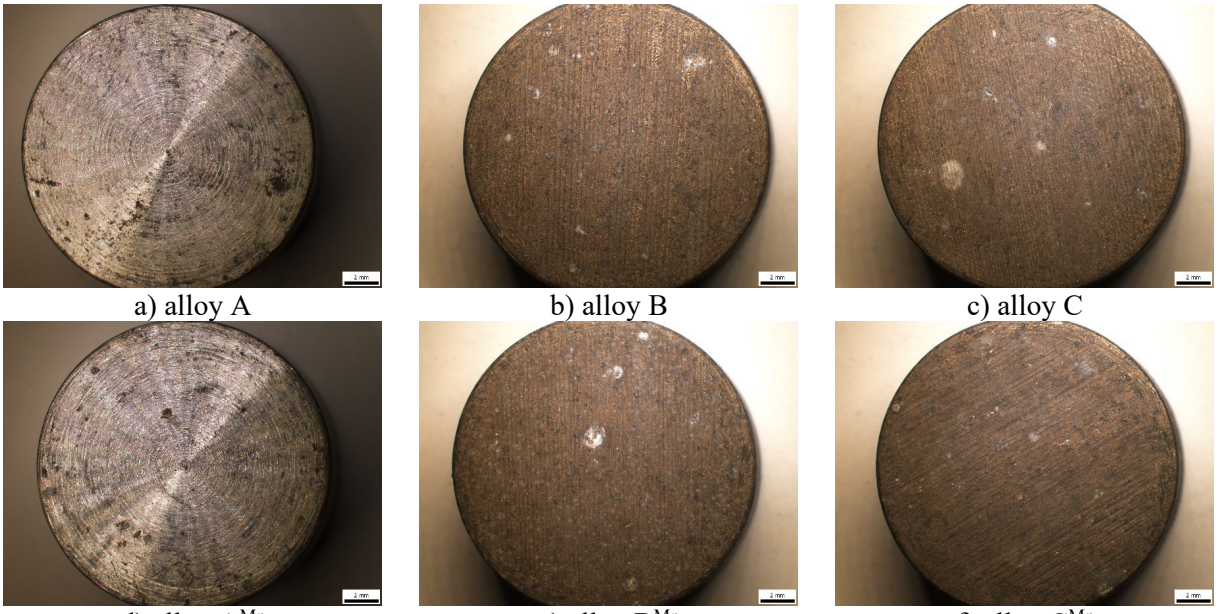

a) alloy A b) alloy B c) alloy C

d) alloy A^{Mn} e) alloy B^{Mn} f) alloy C^{Mn}

Fig.4. *Macrographs of experimental samples after immersion corrosion test a), b), c) – alloys without Mn addition; d), e), f) – with Mn addition.*

However, it cannot be claimed that the level of corrosion attack increased with increasing Fe content in each melt. In the melts with Mn addition, the observed surface was less attacked compared to the samples without Mn addition. Alloy A showed the most severe corrosion damage, with the largest and deepest pits, regardless of the Mn addition (Fig. 4a, d).

It can be observed in the cross-section of the test specimens that the pitting corrosion propagates to the depth of the material through the α-phase in the eutectic.

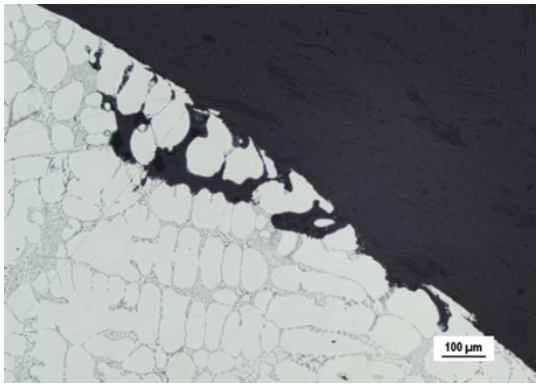

Fig.5. *Presence of pitting corrosion in experimental alloy C.*

Conclusion

The study aimed to determine the impact of increased Fe content and Mn addition on the microstructure and corrosion resistance of AlSi7Mg0.3 cast aluminium alloys after heat treatment T6. The results led to the following conclusions:

- The AlSi7Mg0.3 experimental alloys microstructure is composed of α-phase eutectic and various intermetallic phases such as Fe-rich needle-like Al_5FeSi skeleton-like $Al_{15}(FeMn)_3Si_2$ and Mg_2Si.
- Quantitative analysis revealed that in experimental alloys with Mn addition, there were on average shorter Fe phases. The smallest average length was measured in alloys B^{Mn} and C^{Mn}. Presumably, because the Mn/Fe ratio is close to 0.5.
- The immersion test using 3.5% NaCl was performed in order to evaluate the influence of Mn addition on alloys after heat treatment. The test revealed that in the samples that had Mn addition, the observed surface was less attacked compared to the samples without Mn addition.
- The macrographs of the experimental samples showed pitting corrosion as the type of corrosion that attacked the samples.
- It can be said that Mn addition overall increases corrosion resistance and reduces the size and amount of Fe-rich intermetallic phases even in the alloys after the heat treatment.

Acknowledgements

The research was supported by Grand Agency of Ministry of Education of Slovak Republic and Slovak Academy of Sciences, project KEGA 004ŽU-4/2023, project to support young researchers at UNIZA, ID project 12715 (Kuchariková) and project 313011ASY4 “Strategic implementation of additive technologies to strengthen the intervention capacities of emergencies caused by the COVID-19 pandemic”.

References

[1] D. Varshney, K. Kumar. Application and use of different aluminium alloys with respect to workability, strength and welding parameter optimization, Ain Shams Eng. J. 12 (2021) 1143-1152. https://doi.org/10.1016/j.asej.2020.05.013

[2] F. Czerwinski. Thermal Stability of Aluminum Alloys, Materials 13 (2020) art.3441. https://doi.org/10.3390/ma13153441

[3] L. Lattanzi et al. Room Temperature Mechanical Properties of A356 Alloy with Ni Additions from 0.5 Wt to 2 Wt%, Metals 8 (2018) art.224. https://doi.org/10.3390/met8040224

[4] E. Erzi et al. Determination of Acceptable Quality Limit for Casting of A356 Aluminium Alloy: Supplier’s Quality Index (SQI), Metals 9 (2019) art.957. https://doi.org/10.3390/met9090957

[5] D. Manickam et al. Effect of Solution Heat Treatment and Artificial Aging on Compression Behaviour of A356 Alloy, Medziagoryra 25 (2019) 281-285. https://doi.org/10.5755/j01.ms.25.3.20442

[6] H. Nunes et al. Adding Value to Secondary Aluminum Casting Alloys: A Review on Trends and Achievements, Materials 16 (2023) art.895. https://doi.org/10.3390/ma16030895

[7] L. Stanček et al. Structure and properties of silumin castings solidified under pressure after heat treatment. Met. Sci. Heat Treat. 56 (2014) 197-202. https://doi.org/10.1007/s11041-014-9730-0

[8] B. Vanko, L. Stanček. Utilization of heat treatment aimed to spheroidization of eutectic silicon for silumin castings produced by squeeze casting. Arch. Foundry Eng. 12 (2012) 111-114. https://doi.org/10.2478/v10266-012-0021-1

[9] T. Xu et al. Microstructure and mechanical properties of in-situ nano γ-Al_2O_{3p}/A356 aluminum matrix composite, J. Alloys Compd. 787 (2019) 72-85. https://doi.org/10.1016/j.jallcom.2019.02.045

[10] W.S. Ebhota, J. Tien-Chien. Effects of Modification Techniques on Mechanical Properties of Al-Si Cast Alloys, In: S. Sivasankaran (Ed.), Aluminium Alloys – Recent Trends in Processing, Characterization, Mechanical Behavior and Applications, IntechOpen, 2017. https://doi.org/10.5772/intechopen.70391

[11] M.S. Kaiser et al. Study of Mechanical and Wear Behaviour of Hyper-Eutectic Al-Si Automotive Alloy Through Fe, Ni and Cr Addition, Mater. Res. 21 (2018) art.e20171096. https://doi.org/10.1590/1980-5373-MR-2017-1096

[12] M.A. Moustafa. Effect of iron content on the formation of β-Al5FeSi and porosity in Al-Si eutectic alloys, J. Mater. Proces. Technol. 209 (2009) 605-610. https://doi.org/10.1016/j.jmatprotec.2008.02.073

[13] J. Kozana et al. The Effect of Tin on Microstructure and Properties of the Al-10 wt.% Si Alloy, Materials 15 (2022) art.6350. https://doi.org/10.3390/ma15186350

[14] A.Y. Algendy et al. Formation of intermetallic phases during solidification in Al-Mg-Mn 5xxx alloys with various Mg levels, MATEC Web of Conf. 326 (2020) art.02002. https://doi.org/10.1051/matecconf/202032602002

[15] C. Berlanga-Labari et al. Corrosion of Cast Aluminum Alloys: A Review, Metals 10 (2020) art.1384. https://doi.org/10.3390/met10101384